Journal of Hazardous Materials, 16 (1987) 411–425
Elsevier Science Publishers B.V., Amsterdam — Printed in The Netherlands

THE HEAVY GAS MIXING PROCESS IN STILL AIR AT THORNEY ISLAND AND IN THE LABORATORY

A.P. VAN ULDEN

Royal Netherlands Meteorological Institute, P.O. Box 201, 3730 AE De Bilt (The Netherlands)

(Received November 24, 1986; accepted February 16, 1987)

Summary

A dynamic integral model is described that includes a time dependent radial momentum budget and a turbulent kinetic energy budget. These budgets are used to predict radial gravity spreading and cloud generated turbulent entrainment. In a comparison with measurements it appears that the model accurately describes radial gravity spreading. The measured area-averaged concentrations from the Thorney Island Trials 12 and 34 and from the laboratory experiments by Havens and Spicer [1] are analysed. Evidence is provided that measured concentrations depend strongly and systematically on the measuring height. This implies two things: first, the height of the center of mass of the cloud was not great in comparison with the measuring heights; and second, the "true" surface concentrations are likely to be significantly higher than the concentrations measured at Thorney Island and in the bulk of the laboratory experiments. From the measured data a preliminary normalized concentration profile is deduced. When this profile is used in our model a fair and consistent simulation of the measured concentrations is obtained, both for the two Thorney Island trials and for the laboratory experiments.

1. Introduction

In this paper the heavy gas mixing process is analysed for Thorney Island experimental conditions and for the laboratory experiments in still air by Havens and Spicer [1]. In the Thorney Island experiments large dense clouds were released instantaneously, with an initial volume of about 2000 m^3 and an initial density about twice that of air. In conditions with low atmospheric turbulence such clouds spread rapidly over the ground and soon become wide and shallow. The same is true for the laboratory experiments. Observations show that the radial cloud edge remains distinct for a long time, while the interface at the cloud top is diffuse. This indicates that vertical mixing is the dominant mixing process.

This paper deals with the phase in which mixing by cloud generated turbulence is the dominant mixing process and the radial gravity spreading the dominant radial spreading process. These processes will be described by means of a dynamic integral model and by an analysis of experimental data.

0304-3894/87/$03.50

2. The model

A model for the spreading and mixing of a dense cloud in still air has been described in detail by Van Ulden [2]. This model will be used here and is summarized below.

The cloud dimensions are defined by means of its radius R and its volume V. The cloud radius is obtained by numerical integration with respect to time of the rate equation:

$$dR/dt = U_f \tag{2.1}$$

The front velocity U_f is derived by numerical integration of an equation for dU_f/dt that we have derived from the radial momentum budget of the cloud. This equation will be given later.

The time rate of change of the cloud volume is modeled as

$$dV/dt = \pi R^2 W_e \tag{2.2}$$

where W_e is an entrainment velocity. We neglect edge entrainment and describe W_e by means of the entrainment model by Driedonks and Tennekes [3]. This model reads:

$$W_e = c_e \bar{u}_t / (c_t + Ri_t) \tag{2.3}$$

where $c_e = 0.2$ and $c_t = 1.5$ are empirical coefficients given by the authors,

$$Ri_t = g\,\overline{\Delta\rho}\,H/\bar{\rho}\,\bar{u}_t^{\,2} \tag{2.4}$$

is a bulk turbulent Richardson number, g the acceleration by gravity, $\overline{\Delta\rho}$ the mean density difference between cloud and air, H the cloud height, $\bar{\rho}$ the mean cloud density and $\bar{u}_t$ a bulk turbulent velocity scale defined by the total turbulent kinetic energy T_E in the entraining turbulent layer. In the present flow configuration this corresponds with the following definition

$$\bar{u}_t = (2T_E/\bar{\rho}\,V)^{1/2} \tag{2.5}$$

or

$$T_E = \frac{1}{2}\,V\bar{\rho}\,\bar{u}_t^{\,2} \tag{2.6}$$

In the present model T_E is obtained by numerical integration of an equation for dT_E/dt that we have derived from the energy budget in the cloud. Also this equation will be given later.

Given the cloud dimensions R and V some other important variables can be obtained from simple diagnostic equations. The cloud height is defined as:

$$H \equiv V/\pi R^2 \tag{2.7}$$

The average density difference between cloud and air is obtained from

$$\overline{\Delta\rho} = \Delta\rho_0\ V_0/V \tag{2.8}$$

where $\Delta\rho_0$ and V_0 are the initial values of $\overline{\Delta\rho}$ and V and where we have used that the total mass surplus $\overline{\Delta\rho}\, V$ is a conserved quantity for an isothermal cloud [4]. The average cloud density is given by

$$\bar{\rho} = \rho_a + \overline{\Delta\rho} \tag{2.9}$$

where ρ_a is the air density.
The cloud averaged concentration by volume is defined as

$$\bar{c} = V_0/V \tag{2.10}$$

Because vertical mixing occurs, the assumption of a uniform vertical profile is not adequate for describing concentration. In the present model we do not resolve radial variations in the vertical structure, but we do allow for non uniform vertical concentration profiles. In general the area averaged concentration $c(z)$ can be described by profiles of the type

$$c(z)/\bar{c} = f(z/H) \tag{2.11}$$

where z is the height above the surface and $f(z/H)$ a function of the scaled height z/H, that has to satisfy the following constraints. In the first place the total volume of dense gas should be conserved. This implies:

$$\int_0^\infty \mathrm{f}(z/H)\ \mathrm{d}(z/H) = 1 \tag{2.12}$$

Furthermore this function has to be consistent with the definition of H, which we take in the present paper as:

$$\mathrm{H} \equiv 2\int_0^\infty z\, c(z)\ \mathrm{d}z \Big/ \int_0^\infty c(z)\ \mathrm{d}z \tag{2.13}$$

Thus H is defined as twice the height of the centre of mass of the cloud. It should be noted that this definition for H is consistent with the definition for H used in the entrainment model by Driedonks and Tennekes [3]. Thus eqns. (2.13) and (2.7) are equivalent definitions for H.

Candidates for the scaled concentration profiles (eqn. 2.11) are profiles of the family

$$c(z)/\bar{c} = A \exp\left[-(Bz/H)^s\right] \tag{2.14}$$

where s is a profile shape factor and where

$$A = 2s\,\Gamma(2/s)/[\Gamma(1/s)]^2 \tag{2.15A}$$

and

$$\mathrm{B} = 2\,\Gamma(2/s)/\Gamma(1/s) \tag{2.15B}$$

Γ is the gamma function. This profile family satisfies eqns. (2.12) and (2.13). Furthermore profiles from this family have been observed [5] and can be obtained as solutions of the diffusion equation [6–9]. The family includes the uniform profile ($s=\infty$, $A=1$, $B=2$), the gaussian profile ($s=2$, $A=4/\pi$, $B=2/\sqrt{\pi}$), and the exponential profile ($s=1, A=2, B=2$).

It should be noted that the present model, being an integral model, cannot solve explicitly for the concentration profile. Our model only computes bulk quantities like H and $\bar{c}$. The translation of these quantities into concentration profiles has to be made with an empirical choice for $f(z/H)$. This will be a matter of discussion in Section 3. Here we continue with a description of the momentum budget and the energy budget of the cloud that have to provide us with equations for $\mathrm{d}U_\mathrm{f}/\mathrm{d}t$ and $\mathrm{d}T_\mathrm{E}/\mathrm{d}t$. The equation for $\mathrm{d}U_\mathrm{f}/\mathrm{d}t$ is obtained from the radial momentum budget of the cloud. This budget can be written as [4]:

$$\mathrm{d}M_\mathrm{r}/\mathrm{d}t = F_\mathrm{s} + F_\mathrm{d} + F_\mathrm{a} + F_\mathrm{v} \tag{2.16}$$

where M_r: the radial momentum-integral of the cloud, F_s: the static pressure force due to the negative buoyancy of the cloud, F_d: the drag force on the edge of the cloud due to the presence of quiescent ambient fluid, F_a: the force due to the reaction of ambient fluid to outward radial accelerations of the cloud edge, and F_v: the force due to vertical accelerations in the cloud and the reaction of the ambient fluid to vertical accelerations of the top of the cloud.

In this momentum-budget surface-friction is neglected.

Van Ulden [2] showed that from this momentum budget the following equation for the front velocity can be derived:

$$\frac{\mathrm{d}U_\mathrm{f}}{\mathrm{d}t} = \frac{g\overline{\Delta\rho}\frac{H}{R} - \left[c_\mathrm{d} - 6\frac{H}{R} - 4\frac{\bar{\rho}}{\rho_\mathrm{a}}\left(\frac{H}{R}\right)^2\right]\frac{\rho_\mathrm{a} U_\mathrm{f}^2}{R} - \left[\frac{2}{3} + 6\frac{H}{R} + \frac{4}{3}\left(\frac{\bar{\rho}}{\rho_\mathrm{a}} + 2\right)\left(\frac{H}{R}\right)^2\right]\frac{\rho_\mathrm{a} W_\mathrm{e} U_\mathrm{f}}{H}}{\frac{2}{3}\bar{\rho} + 4\rho_\mathrm{a}\frac{H}{R} + \frac{4}{3}\bar{\rho}\left(\frac{H}{R}\right)^2} \tag{2.17}$$

In the numerator of this equation we may recognize the following terms: $g\,\overline{\Delta\rho}\,H/R$ representing the static pressure force, $c_\mathrm{d}\,\rho_\mathrm{a}\,U_\mathrm{f}^2/R$ representing the drag force with c_d a drag coefficient, and $\frac{2}{3}\rho_\mathrm{a} W_\mathrm{e} U_\mathrm{f}/H$ representing the radial stress. The other terms containing H/R represent the effect of cloud deformation on the contribution of acceleration reactions to $\mathrm{d}U_\mathrm{f}/\mathrm{d}t$. These terms are present because H/R is continuously changing due to slumping and entrainment. Similarly the term containing $(H/R)^2$ gives the effect of cloud deformation on the contribution to $\mathrm{d}U_\mathrm{f}/\mathrm{d}t$ of vertical accelerations inside the cloud.

The denominator gives the inertial terms of the radial momentum inside the

cloud, of the virtual momentum outside the cloud and of the vertical momentum inside the cloud, respectively. This last term is the major inertial term when $\bar{\rho}/\rho_a$ is large and $(H/R)=2$, as in the Thorney Island experiments. It is thus clear that this term should not be omitted in a dynamic model. Therefore models based on the shallow layer approximation are not likely to behave well in the early spreading stages.

In the derivation of eqn. (2.17) Van Ulden [2] used the following parameterization of the drag force:

$$F_a = c_d \pi R H \rho_a U_f^2 \tag{2.18}$$

with the drag coefficient taken constant and obtained by fitting the model to the experimental data of Havens and Spicer [1]. This may be not fully satisfactory because the cloud height H_f near the leading edge may be significantly lower or greater than the mean cloud height H. Therefore it is better to parameterize the drag force as:

$$F_a = c_d' \pi R H_f \rho_a U_f^2 \tag{2.19}$$

as proposed by Van Ulden [4]. H_f and c_d' can be found by using the leading edge conditions [4]:

$$U_f/(g \overline{\Delta\rho} H_f/\rho_a)^{1/2} \simeq 1.15 \tag{2.20}$$

and

$$c_d' \simeq 0.84 \tag{2.21}$$

These values have been obtained from laboratory data (e.g. [10]) and are valid for frontal Reynolds numbers $U_f H_f/\nu > O(10^3)$. Using these leading edge conditions implies that we model the drag coefficient in eqn. (2.18) as

$$c_d = 0.64 \rho_a U_f^2 / g \overline{\Delta\rho} H \tag{2.22}$$

Thus c_d now depends on the model variables U_f, $\overline{\Delta\rho}$ and H.

The equation for dT_E/dt is derived from the conservation of total energy in a large control volume containing the cloud and the secondary flows around it. In the present problem we distinguish between four types of energy: the potential energy P_E, the kinetic energy of mean radial and vertical motions K_E, the earlier mentioned turbulent kinetic energy T_E and the internal heat I_E. The conservation law reads

$$\frac{d}{dt}(P_E + K_E + T_E + I_E) = 0 \tag{2.23}$$

Between the various forms of energy four transformation processes take place. Namely:

- the rate G, at which gravity transforms potential energy into mean kinetic energy,

- the buoyant destruction B of turbulent energy, which is the conversion of turbulent energy into potential energy by entrainment,
- the shear production S of turbulent energy, and
- the dissipation D of turbulent energy into internal heat.

The equations for this system are:

$$dP_E/dt = -G+B \tag{2.24}$$

$$dK_E/dt = G-S \tag{2.25}$$

$$dT_E/dt = S-B-D \tag{2.26}$$

and

$$dI_E/dt = D \tag{2.27}$$

By parameterizing S, B and D Van Ulden [2] obtained the following equation for the cloud generated turbulent energy:

$$\frac{dT_E}{dt} = c_d \rho_a V \frac{U_f^3}{R} + \left[\frac{1}{3} + 2\frac{H}{R} + 2\left(\frac{H}{R}\right)^2\right] \rho_a V \frac{W_e U_f^2}{H} - \frac{c_n \bar{\rho} V \bar{u}_t^3}{H} - \frac{(c_b+1)\, c_e g \Delta\rho_0 V_0 \bar{u}_t}{2(c_t + Ri_t)} \tag{2.28}$$

In this equation the first two terms at the right hand side give the production of turbulent energy. In these terms we can identify $c_d \rho_a V U_f^3/R$ as the production at the cloud edge, earlier proposed by Van Ulden [4], and $\frac{1}{3}\rho_a V W_e U_f^2/H$ as the shear production at the cloud top. The terms containing H/R and $(H/R)^2$ represent the additional shear production related to secondary flows.

The latter two terms in eqn. (2.28) represent the dissipation and buoyant destruction of turbulent energy. In these terms

$$c_n = 0.1 \tag{2.29}$$

and

$$c_b = 2.0 \tag{2.30}$$

are numerical coefficients for the dissipation terms. These values correspond with the assumption of a critical flux Richardson number $Ri_c \equiv B/(B+D) = 0.25$. With these results we have completed our model summary. In total we have obtained a closed set of 4 rate equations (2.1), (2.2), (2.17) and (2.28) and a number of diagnostic equations (2.3)–(2.15). This set can be solved with standard numerical methods. It should be noted that in our model all numerical coefficients have been estimated independently of the experiments that we will analyse in the following section.

TABLE 1

Experiments by Havens and Spicer [1]

$\Delta\rho_0/\rho_a = 3.19$, $H_0/R_0 = 2$						
Symbol used in figures	●	△	◇	○	+	×
V_0 [m^3]	0.531	0.135	0.535	0.054	0.054	0.054
z_m/H_0	0.007	0.011	0.015	0.015	0.049	0.098

3. Analysis and simulation of still air experiments

3.1. Experimental characteristics

In this section we analyse laboratory experiments by Havens and Spicer [1] and Thorney Island trials with low atmospheric turbulence. The characteristics of the experiments we use from Havens and Spicer are given in Table 1. As we see, the initial volumes vary by a factor of 10, while the measuring heights used vary by a factor 14. So possible effects of scale and measuring height can be investigated.

From Thorney Island we select the Trials 12 and 34, because these were trials with a low atmospheric turbulence as expressed by its density

$$t_E \equiv \tfrac{1}{2}\rho_a \ (\sigma_u{}^2 + \sigma_v{}^2 + \sigma_w{}^2) \tag{3.1}$$

where $\sigma_u{}^2$, $\sigma_v{}^2$ and $\sigma_w{}^2$ are the variances of the three wind components. We approximate this turbulent kinetics energy density by

$$t_E = \tfrac{1}{2}\rho_a \ (c_* \, u_*)^2 \tag{3.2}$$

where u_* is the surface friction velocity and

$$c_* \simeq 3 \tag{3.3}$$

an empirical coefficient [11,12]. The friction velocity u_* can be estimated from the windpspeed U_{10} at 10 m, the surface roughness length z_0 and the cloud cover using a procedure by Van Ulden and Holtslag [13]. For our calculation we used zero cloud cover, $z_0 = 0.01$ m and the observed windspeeds. The resulting u_* is given in Table 2. This result will be used later to estimate the period in which atmospheric turbulence presumably has a negligible effect on cloud mixing. The other experimental characteristics of the Trials 12 and 34 are also given in Table 2.

3.2 Analysis and simulation of radial spreading

Havens and Spicer [1] provide accurate measurements of the cloud radius as a function of time. For the Thorney Island Trials 12 and 34, no such data are available. Thus in this section we only analyse the laboratory data. To

TABLE 2

Thorney Island trials

Trial no.	12	34
Symbol used in figures	C	S
$\Delta\rho_0/\rho_a$	1.37	0.83
H_0/R_0	1.81	1.95
V_0 [m^3]	1950	2100
z_m/H_0	0.032	0.029
U [m s^{-1}]	2.6	1.4
u_* [m s^{-1}]	0.080	0.028

investigate possible scale effects we non-dimensionalize the data with the initial radius R_0 and the velocity scale

$$U_0 \equiv (g\,\Delta\rho_0\,H_0/\rho_a)^{1/2} \tag{3.4}$$

where H_0 is the initial cloud height.
The time is scaled with

$$t_0 = R_0/U_0 \tag{3.5}$$

In Fig. 1 we give the experimental data on dimensionless cloud area, together with our model simulation. As we see there appears to be no scale effect in the data and viscous effects do not seem to be present for the time interval shown. The performance of the model is quite satisfactory. The time delay connected with the initial acceleration is well modeled. The straight part of the curve corresponds with

$$k \equiv U_r/(g\overline{\Delta\rho}\,H/\rho_a)^{1/2} = 1.20 \tag{3.6}$$

This result agrees very well with the average Froude number $K = 1.19$ that was observed for the Thorney Island Trials 8, 9 and 10 [14]. These are trials with moderately low windspeeds.

3.3 Analysis and simulation of the mixing process

In this section we will analyse and simulate area-averaged concentrations. For the Thorney Island trials pertinent data are available [15,16]. For the laboratory experiments we have computed area averages from the graphs given in the report [1]. The contribution to the average of each sensor was weighted according to the area for which the sensor is representative. The representative area scales with $2\pi\,r_m\,\Delta r$, where r_m is the distance of the sensor from the origin and Δr the spacing between the sensors. Thus the present analysis puts more weight on the outer sensors. For greater times this leads to area-averaged concentrations that are only slightly lower than the values given by Van Ulden

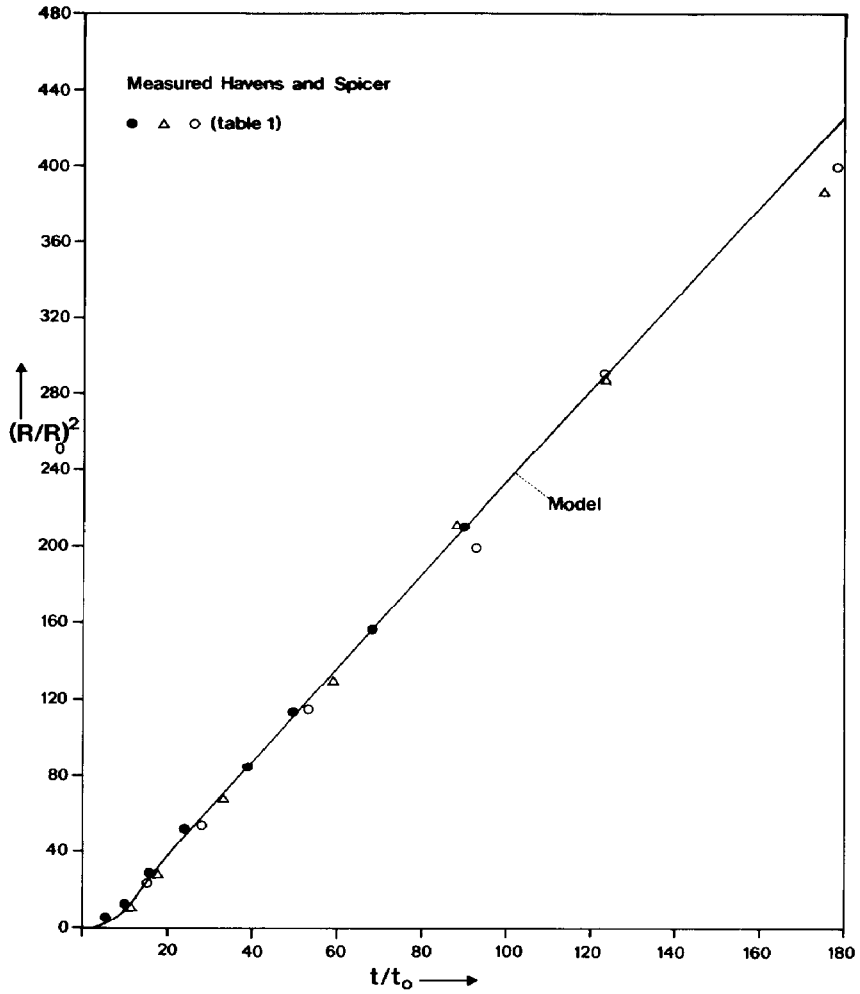

Fig. 1. Observed and predicted dimensionless cloud area $(R/R_0)^2$ against dimensionless time t/t_0. Data from Havens and Spicer [1]. Explanation of symbols is given in Table 1.

[2]. We further require that at least three sensors saw gas and that the cloud did not move too far beyond the outermost sensor. This reduces the r.m.s. error of the computed area-averages to about 10–20% and limits the period of reliable data to the dimensionless time interval $30 < t/t_0 < 180$. This time interval will be included in the analysis.

The Thorney Island data, which cover a much longer period can only be used in the present analysis, as long as mixing by atmospheric turbulence can be neglected. We assume that this is the case when the atmospheric turbulent energy density is less than half the turbulent energy density produced by the cloud as computed with our model. This is the case in Trial 12 for $t/t_0 < 70$ and

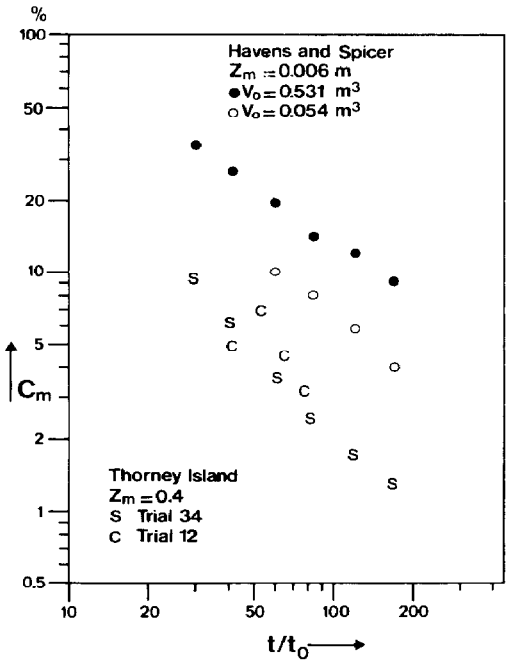

Fig. 2. Observed area-averaged concentration c_m against dimensionless time t/t_0. Symbols as in Tables 1 and 2.

in Trial 34 for $t/t_0 < 170$. Thus we include in our analysis only data from the Thorney Island trials for dimensionless times smaller than these limits.

After this careful data selection, we now proceed with a comparison between the various experiments. A representative selection is shown in Fig. 2. Included are data from Havens and Spicer [1] for $V_0 = 0.531$ m^3 and $V_0 = 0.054$ m^3. Further we give the data for the Thorney Island Trials 12 and 34. In the figure we see very significant differences between the experiments. The question is: what causes the differences? At first sight one might think that apparently different mixing processes are involved. There is, however, an alternative and quite exciting interpretation. It may be that the measurements depend strongly on the dimensionless measuring height z_m/H_0. Let us investigate this possibility.

In Fig. 3 we have plotted measured area averaged concentrations as a function of this dimensionless measuring height for $t/t_0 = 60$. Apart from 4 data points taken from Fig. 2, we have also plotted data from other laboratory experiments including estimates of the area averaged concentration obtained from sensors put at 0.02 m and 0.04 m. This figure strongly suggests that the observed concentrations decrease rapidly with height. The Thorney Island data are fairly consistent with the trend observed for the laboratory data. Similar figures can be made for different times and a similar behavior is observed. A more com-

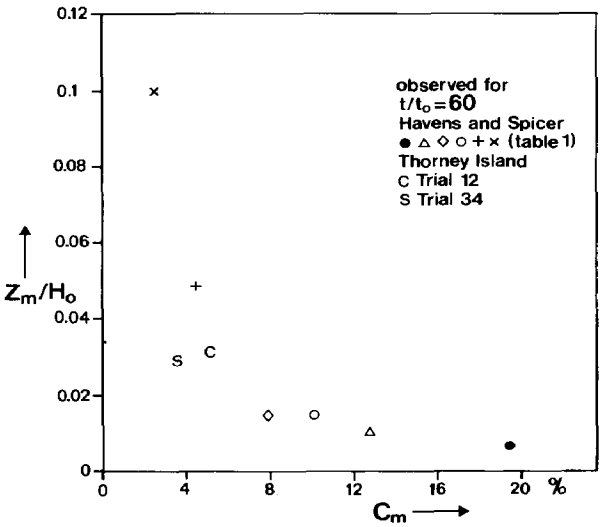

Fig. 3. Observed area-averaged concentration c_m against dimensionless measuring height z_m/H_0, where H_0 is the initial cloud height. Symbols as in Tables 1 and 2.

plete picture of the concentration profile can be obtained by plotting the data for the different times in a scaled form. This is done In Fig. 4. Measured concentrations c_m have been normalized with cloud averaged concentrations $\bar{c}_c$ as calculated with our model. Similarly the measuring height z_m is normalized with the calculated cloud height H_c. The result is that all data appear to show a similar decrease with height. In fact we have plotted the concentration profile in the similarity co-ordinates suggested by eqn. (2.11). The data suggest that such a similarity function exists, at least for the analysed time interval.

For reference purposes we show in the figure the Gaussian profile. It is clear that the concentration profile is not Gaussian. Thus the fair agreement Van Ulden [2] found, between concentrations computed with a Gaussian profile and the data for the experiments with $V_0=0.531$ m^3 is fortuitous. In the figure another curve is shown that more or less goes through the data. This curve is the similarity profile. (eqn. 2.14) with a shape factor $s=1/2$. It reads

$$c(z)/\bar{c}=6 \exp\,[-(12\,z/H)^{1/2}] \tag{3.7}$$

With showing this curve, we do not imply that it gives a correct description of the concentration profile below $z/H=0.1$. In this respect the data are not conclusive. The results of the above analysis may be biased by the use of our model for calculating H_c and $\bar{c}_c$. We think, however, that this bias is weak at the most. The reason is that the data in Fig. 4 show a hyperbolic behaviour in the sense that $z_m\, c_m/H_c\, \bar{c}_c \simeq 0.2$ is approximately constant for the bulk of the data. Since $H_c \bar{c}_c = V_0/\pi R_c{}^2$ and since our model predicts the cloud area quite accurately, errors in the entrainment model lead to compensating errors in H_c and $\bar{c}_c$.

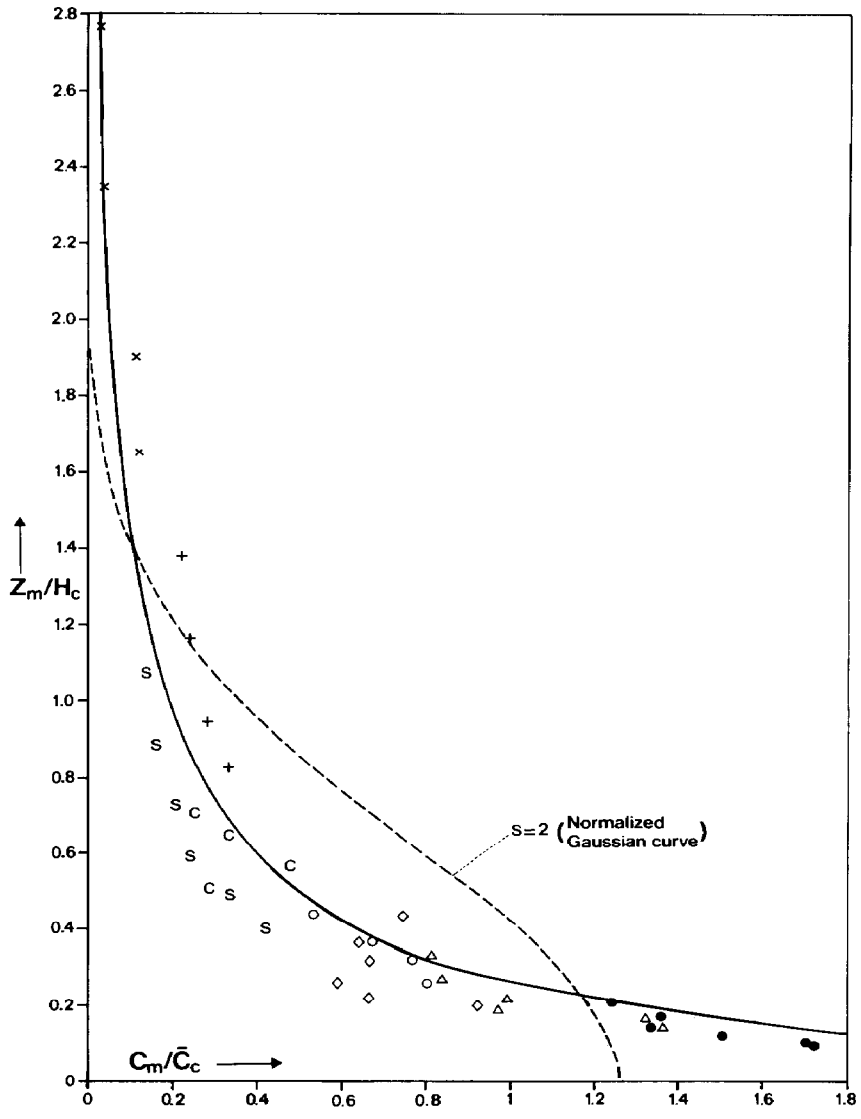

Fig. 4. Observed normalized concentration $c_m/\bar{c}_c$ against normalized measuring height z_m/H_c. Symbols as in Tables 1 and 2. $\bar{c}_c$ is the calculated volume-averaged concentration and H_c the calculated cloud height for the values of t/t_0 shown in Fig. 2. The curves shown are: broken line: $(4/\pi)\ \exp\ [-(4/\pi)\ (z/H)^2]$ (Gaussian curve), solid line: $6\ \exp\ [-(12z/H)^{1/2}]$.

Therefore errors in the entrainment model only give rise to a shift of the data along the fitted curve and have a minor effect on the analysis. In this context it should be noted that the curvature of the vertical concentration profile found here, is also present in the profile analysis by Brighton [15]. This follows from

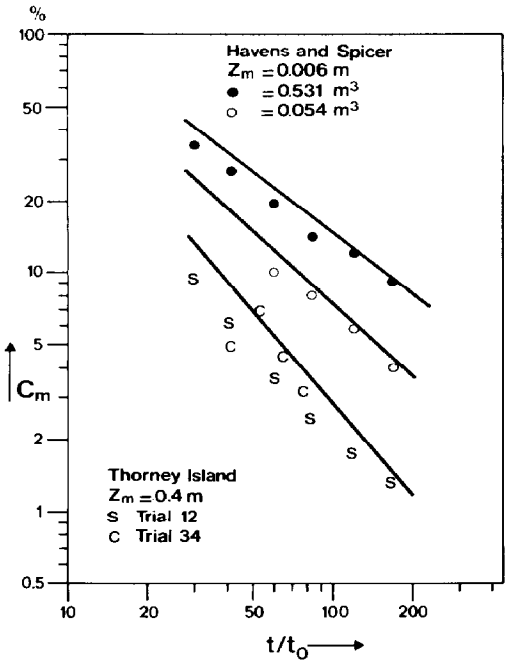

Fig. 5. Observed and predicted area-averaged concentration c_m against dimensionless time (data as in Fig. 2).

the fact that the latter author found negative values of h_p for most of the time (see his section 2.4).

Let us take now eqn. (3.7) as a preliminary estimate of the dimensionless concentration profile and use it in our model to predict the concentrations at the observation heights of the data given in Fig. 2. The result is shown in Fig. 5. In this figure the model results for Trials 12 and 34 approximately coincide and are given by one curve. For the two laboratory experiments both model curves are given. We see that the agreement between the model and the data is satisfactory. Thus making corrections for the observation height removes the discrepancy between the Thorney Island data and the laboratory data and also explains the differences between the two laboratory data sets for different initial volume. The present analysis indicates that no significant viscous effects are present in the laboratory data as suggested earlier by Van Ulden [2].

An important preliminary conclusion is that at least in the low wind speed trials at Thorney Island, the observations at 0.4 m are not representative for the volume averaged concentrations and may be very much less than the not observed surface concentrations. If our interpretation is correct the Thorney Island data need a careful reanalysis. For example the cloud heights as derived

by Brighton [15] may be significantly too high. The same is true for empirical coefficients for side entrainment.

Conclusions

We have presented a dynamical integral model that satisfactorily describes the radial gravity spreading observed in the laboratory. No ad hoc adjustment of empirical coefficients is needed to achieve this result. Also our model gives non-adjustment predictions for the cloud height and the volume averaged concentration. These model predictions in combination with a preliminary empirical similarity profile also simulate the concentrations observed in the laboratory and in the field in "still air" conditions. At the present state this concentration profile is an ad hoc adjustment to the data analysed in this paper.

Evidence is provided that concentrations decrease rapidly with height. This indicates that corrections have to be made for the measuring height when experiments are simulated.

Existing interpretations of the Thorney Island data and the laboratory data may have to be revised, e.g. empirical coefficients for side entrainment used by many others may be too high, as well as the cloud height.

References

1 J.A. Havens and T.O. Spicer, Development of an atmospheric dispersion model for heavier-than-air gas mixtures, Report no. CG-D-23-85, U.S. Coast Guard, Washington, DC, 1985.

2 A.P. van Ulden, The spreading and mixing of a dense cloud in still air, In: J. Puttock (Ed.), Proc. I.M.A. Conference on Stably Stratified Flow and Dense Gas Dispersion, Chester, April 19, 1986, Oxford University Press, in press.

3 A.G.M. Driedonks and H. Tennekes, Environment effects in the well-mixed atmospheric boundary layer, Boundary-Layer Meteorol., 30 (1984) 75–105.

4 A.P. van Ulden, A new bulk model for dense gas dispersion: two-dimensional spread in still air, In: G. Ooms and H. Tennekes (Eds.), Atmospheric Dispersion of Heavy Gases and Small Particles, Springer Verlag, Berlin, 1984, pp. 419–440.

5 F.T.M. Nieuwstadt and A.P. van Ulden, A numerical study on the vertical dispersion of passive contaminants from a continuous source in the atmospheric surface layer, Atmos. Environ., 12 (1978) 2119–2124.

6 P.C. Chatwin, The dispersion of a puff of passive contaminant in the constant stress regfion, Q.J. R. Meteorol. Soc., 94 (1968) 350–360.

7 A.P. van Ulden, Simple estimates of vertical diffusion from sources near the ground, Atmos. Environ., 12 (1978) 2121–2129.

8 J.C.R. Hunt and A.H. Weber, A Lagrangian statistical analysis of diffusion from a ground-level source in a turbulent boundary layer, Q. J. R. Meteorol. Soc., 105 (1979) 423–443.

9 A.P. van Ulden and F.T.M. Nieuwstadt, A discussion, Atmos. Environ., 14 (1980) 269–270.

10 J.E. Simpson and R.E. Britter, The dynamics of the head of a gravity current, advancing over a horizontal surface, J. Fluid Mech., 94 (1979) 477–495.

11 A.C.M. Beljaars, P. Schotanus and F.T.M. Nieuwstadt, Surface layer similarity under non-uniform fetch conditions, J. Climate Appl. Meteorol., 22(10) (1983) 1800–1810.

12 J.S. Puttock, Analysis of meteorological data for the Thorney Island Phase I trials, J. Hazardous Materials, 16 (1987) 43–74.

13 A.P. van Ulden and A.A.M. Holtslag, Estimation of atmospheric boundary layer parameters for diffusion applications, J. Climate Appl. Meteorol., 24(11) (1985) 1196–1207.
14 P.W.M. Brighton, A.J. Prince and D.M. Webber, Determination of cloud area and path from visual and concentration records, J. Hazardous Materials, 11 (1985) 155–178.
15 P.W.M. Brighton, Area-averaged concentrations, height-scales and mass balances. J. Hazardous Materials, 11 (1985) 189–208.
16 P.W.M. Brighton and A.J. Prince, Overall properties of the heavy gas clouds in the Thorney Island Phase II trials, J. Hazardous Materials, 16 (1987) 103–138.